

Structural models of vanadate-dependent haloperoxidases and their reactivity

MANNAR R MAURYA

Department of Chemistry, Indian Institute of Technology, Roorkee 247 667
e-mail: rkmanfcy@iitr.ernet.in

Abstract. Vanadium(V) complexes with hydrazone-based ONO and ONN donor ligands that partly model active-site structures of vanadate-dependent haloperoxidases have been reported. On reaction with $[\text{VO}(\text{acac})_2]$ (Hacac = acetylacetonate) under nitrogen, these ligands generally provide oxovanadium(IV) complexes $[\text{VO}(\text{ONO})\text{X}]$ (X = solvent or nothing) and $[\text{VO}(\text{acac})(\text{ONN})]$, respectively. Under aerobic conditions, these oxovanadium(IV) species undergo oxidation to give oxovanadium(V), dioxovanadium(V) or μ -oxobis{oxovanadium(V)} species depending upon the nature of the ligand. Anionic and neutral dioxovanadium(V) complexes slowly deoxygenate in methanol to give monooxo complexes $[\text{VO}(\text{OMe})(\text{MeOH})(\text{ONO})]$. The anionic complexes $[\text{VO}_2(\text{ONO})]^-$ can also be converted *in situ* on acidification to oxohydroxo complexes $[\text{VO}(\text{OH})(\text{HONO})]^+$ and to peroxo complexes $[\text{VO}(\text{O}_2)(\text{ONO})]^-$, and thus to the species assumed to be intermediates in the haloperoxidase activity of the enzymes. In the presence of catechol (H_2cat) and benzohydroxamic acid (H_2bha), oxovanadium(IV) complexes, $[\text{VO}(\text{acac})(\text{ONN})]$ gave mixed-chelate oxovanadium(V) complexes $[\text{VO}(\text{cat})(\text{ONN})]$ and $[\text{VO}(\text{bha})(\text{ONN})]$ respectively. These complexes are not very stable in solution and slowly convert to the corresponding dioxo species $[\text{VO}_2(\text{ONN})]$ as observed by ^{51}V NMR and electronic absorption spectroscopic studies.

Keywords. Structural models; haloperoxidases; vanadium complexes; reactivity of vanadium complexes.

1. Introduction

Recent interest in vanadium complexes stems from their potential therapeutic^{1–5} and catalytic applications.^{6–11} Modelling the structure and properties of vanadium-containing molecules have also influenced research on vanadium chemistry. Examples of interest in this context are the vanadate-dependent haloperoxidases^{12,13} and vanadium nitrogenases.^{14,15} Vanadate-dependent haloperoxidase enzymes e.g. *Ascophyllum nodosum* (isolated from brown algae),¹⁶ *Corallina officinalis* (from red algae),¹⁷ and *Curvularia inaequalis* (from fungi)¹⁸ have been structurally characterized and all of these show a high degree of amino acid homology in their active centres and thus have almost identical active site structures as shown in figure 1 for *Ascophyllum nodosum* as an example.

In these enzymes vanadium is covalently linked to the N^ϵ of an imidazolyl moiety of proximal histidine and to the axial OH group *trans* to the histidine which is further hydrogen-bonded to a distal (“catalytic”) histidine and to water molecules. The overall geometry is trigonal bipyramidal with O_4N coordi-

nation. On coordination with peroxide (O_2^{2-}), they form peroxo complexes where the axial (proximal) histidine moves to a basal position giving rise to a tetragonal $\{\text{VO}(\text{O}_2)(\text{OH})(\text{His})\}$ pyramid with the peroxo ligand occupying two equatorial positions in the symmetrical side-on manner.¹⁹ The peroxo form has also been structurally characterized for the fungal *Curvularia inaequalis*.²⁰

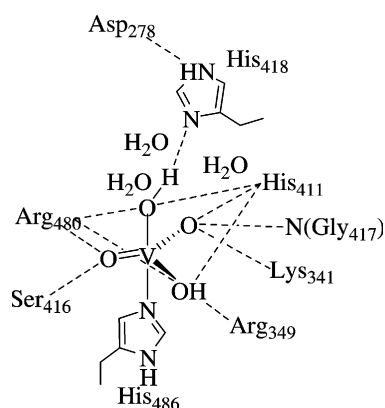
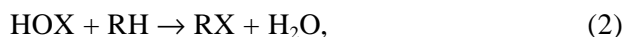
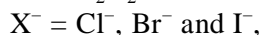
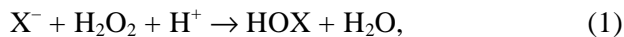


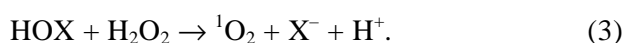
Figure 1. Active site structure of vanadate-dependent haloperoxidase from *Ascophyllum nodosum*.

These enzymes catalyse the oxidation of halides (X^-) to hypohalous acid (HOX) according to (1) below, using H_2O_2 as an oxidant followed by non-enzymatically halogenation of organic compounds.^{21,22}

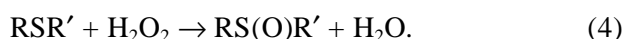


RH = organic substrate, RX = halogenated product.

Without a suitable organic substrate, the two-electron oxidation of halide may result in production of singlet oxygen,



They also oxidize (prochiral) sulphide to (chiral) sulphoxide, as^{23,24}

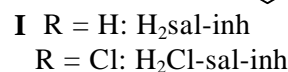
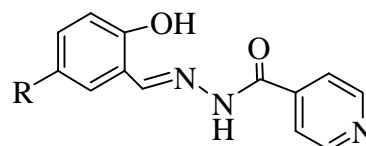


Intermediate species having $\{VO(H_2O)\}$, $\{VO_2\}$, $\{VO(OH)\}$ and $\{VO(O_2)\}$ cores have been postulated during catalytic turnover. The stability of vanadium(V) complexes under aerobic conditions has allowed the design of structural and/or functional models for the haloperoxidases and to isolate or generate species with the above group in solution.²⁵ In this report, we briefly discuss our recent efforts in designing structural models for haloperoxidases. Reactivity of the resulting complexes with various substrates has also been carried out to explore the other aspects of these complexes.

2. Structural models of haloperoxidases

2.1 Complexes with dianionic ONO donor ligands

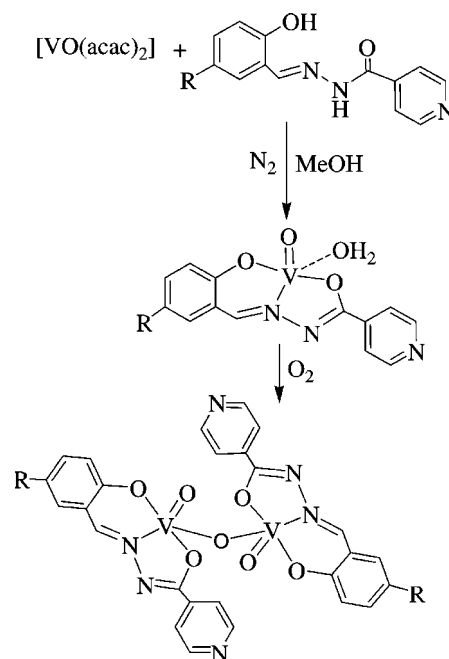
The dioxovanadium(V) complexes $[K(H_2O)][VO_2(\text{sal-inh})]$ ($H_2L = \mathbf{I}$, $R = H$) and $[K(H_2O)][VO_2(\text{Cl-sal-inh})]$ ($H_2L = \mathbf{I}$, $R = Cl$) have been isolated by the reaction of potassium vanadate(V), prepared *in situ* by dissolving V_2O_5 in aqueous KOH, and potassium salt of ligands \mathbf{I} at $pH \approx 7.5$. The final pH of the reaction mixture plays an important role in that a decrease in pH (to ≈ 6.5) causes the formation of oxo-bridged binuclear complexes $[\{VO(\text{sal-inh})\}_2\mu-O]$ and $[\{VO(\text{Cl-sal-inh})\}_2\mu-O]$ along with the respective anionic species. These anionic and neutral complexes can be separated by fractional crystallization where binuclear complex crystallizes out first.



Similarly, reaction of $NH_4[VO_3]$ and the sodium salt of $H_2\text{sal-inh}$ results in the formation of the corresponding ammonium salt $NH_4[VO_2(\text{sal-inh})(H_2O)]$ and $[\{VO(\text{sal-inh})\}_2\mu-O]$. The binuclear complexes have also been synthesized by allowing equimolar amounts of $[VO(\text{acac})_2]$ and ligand to react in acetone, followed by aerial oxidation as shown in scheme 1. Intermediate oxovanadium(IV) complexes $[VO(\text{sal-inh})(H_2O)]$ and $[VO(\text{Cl-sal-inh})(H_2O)]$ can also be isolated as a stable solid.²⁶

The existence of two sharp bands in the $900\text{--}950\text{ cm}^{-1}$ in dioxovanadium(V) complexes suggests a *cis*- VO_2 arrangement. In binuclear complexes, one sharp band arises at $\approx 960\text{ cm}^{-1}$, assignable to $\nu(V=O)$, and a broad band is observed at $\approx 860\text{ cm}^{-1}$ due to $\nu[V-(\mu-O)-V]$. All the complexes display an intense to medium electronic spectral band at $403\text{--}410\text{ nm}$ which is assigned to ligand-to-metal charge transfer (LMCT) transition from phenolate oxygen atom to an empty *d*-orbital of the vanadium atom.

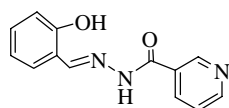
^{51}V NMR spectroscopy has been proved to be an important technique to investigate interaction of va-



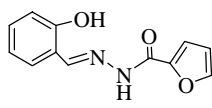
Scheme 1.

niadium(V) with organic ligands. The dioxovanadium(V) complexes show one strong resonance between -539 and -550 ppm in DMSO- d_6 due to coordination of mixed O/N donor ligands. However, owing to the quadrupolar interaction (for ^{51}V nucleus: nuclear spin = $7/2$, quadrupole moment = $-0.05 \times 10^{-28} \text{ m}^2$), the resonances are somewhat broadened; the line widths at half-height are approximately 200 Hz, which is still relatively narrow in ^{51}V NMR spectroscopy.²⁷

Anionic and neutral μ -oxo binuclear complexes of the types $[\text{VO}_2\text{L}]^-$ and $[(\text{VOL})_2\mu\text{-O}]$ (H_2L = ligands) with ligands **II** ($\text{H}_2\text{sal-nah}$) and **III** ($\text{H}_2\text{sal-fah}$) have also been isolated similarly as reported above.²⁸



II: $\text{H}_2\text{sal-nah}$



III: $\text{H}_2\text{sal-fah}$

Neutral complexes $[\{\text{VO}(\text{sal-nah})\}_2\mu\text{-O}]$ and $[\{\text{VO}(\text{sal-fah})\}_2\mu\text{-O}]$ are stable in the solid state, but undergo deoxygenation slowly in methanol to give $[\text{VO}(\text{OMe})(\text{MeOH})(\text{sal-nah})]$ and $[\text{VO}(\text{OMe})(\text{MeOH})(\text{sal-fah})]$ respectively. Molecular structures of these oxo-methoxo complexes are presented in figure 2. The coordination geometry around vanadium can be described as tetragonal bipyramidal, with the doubly bonded oxygen and methanol in axial

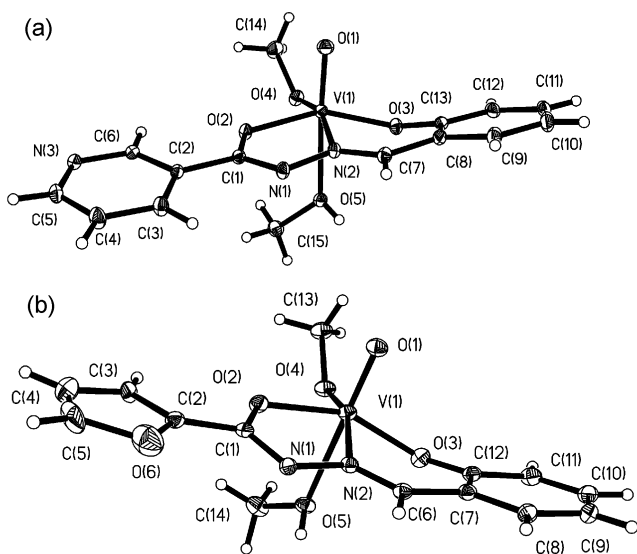


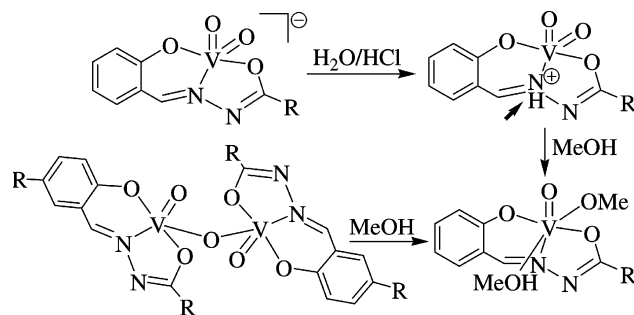
Figure 2. ORTEP plot (at 50% probability level) of $[\text{VO}(\text{OMe})(\text{MeOH})(\text{sal-nah})]$ (a) and $[\text{VO}(\text{OMe})(\text{MeOH})(\text{sal-fah})]$ (b).

positions. The $\text{O}=\text{V}-\text{O}$ (methanol) axis is almost linear; the angle at vanadium is $175.39(5)^\circ$ in $[\text{VO}(\text{OMe})(\text{MeOH})(\text{sal-nah})]$ and $173.4(2)^\circ$ in $[\text{VO}(\text{OMe})(\text{MeOH})(\text{sal-fah})]$. Owing to the *trans* influence of the oxo group, the vanadium–methanol distance $\{d(\text{V}-\text{O5})$ of $2.2514(10) \text{ \AA}$ in $[\text{VO}(\text{OMe})(\text{MeOH})(\text{sal-nah})]$ and $2.3081(15) \text{ \AA}$ in $[\text{VO}(\text{OMe})(\text{MeOH})(\text{sal-fah})]\}$ is considerably elongated, making the methanol a weakly coordinated ligand.

Aqueous solutions of $[\text{VO}_2(\text{sal-nah})]^-$ and $[\text{VO}_2(\text{sal-fah})]^-$ react with HClO_4 or HCl to yield the neutral complexes $[\text{VO}_2(\text{Hsal-nah})]$ and $[\text{VO}_2(\text{Hsal-fah})]$ respectively, in which one of the nitrogens of the $-\text{N}=\text{N}-$ group is protonated. Isolation and structural characterization of such complexes, e.g. $[\text{VO}_2(\text{Hsal-bhz})]$, has been reported by Plass *et al.*²⁹ Slow crystallization of $[\text{VO}_2(\text{Hsal-nah})]$ and $[\text{VO}_2(\text{Hsal-fah})]$ from excess methanol causes the removal of the proton from the NH group and conversion to the methoxo-oxovanadium(V) complexes as mentioned above. The formation of the methoxo-oxovanadium(V) complexes from the corresponding neutral mono- or μ -oxo binuclear oxovanadium(V) complexes in methanol is of interest in the context of vanadium complexes used as oxo-transfer agents both in catalytic and stoichiometric oxygenation reactions.³⁰ Scheme 2 presents the whole synthetic procedures.

Reaction between equimolar amounts of $[\text{VO}(\text{acac})_2]$ and ligands **IV** ($\text{H}_2\text{pydx-inh}$), **V** ($\text{H}_2\text{pydx-nah}$) and **VI** ($\text{H}_2\text{pydx-bhz}$) in dry refluxing methanol gave oxovanadium(IV) complexes from which neutral dioxovanadium(V) complexes $[\text{VO}_2(\text{Hpydx-inh})]$, $[\text{VO}_2(\text{Hpydx-nah})]$ and $[\text{VO}_2(\text{Hpydx-bhz})]$ have been isolated on aerial oxidation.³¹

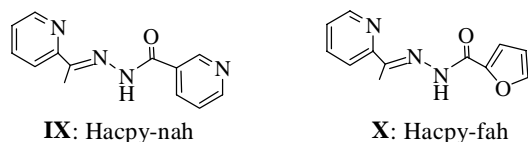
In these complexes, the nitrogen in pyridine is protonated. However, the NH proton signal was not observed in the ^1H NMR spectra of the complexes due



$\text{R} = 3\text{-pyridyl}, 2\text{-furyl}$

Scheme 2.

plexes $[\{\text{VO}(\text{acpy-nah})\}_2(\mu\text{-O})_2]$ and $[\{\text{VO}(\text{acpy-fah})\}_2(\mu\text{-O})_2]$ on oxidation of the methanolic solutions of their corresponding oxovanadium(IV) complexes $[\text{VO}(\text{acac})(\text{acpy-nah})]$ and $[\text{VO}(\text{acac})(\text{acpy-fah})]$.³³ Defflon *et al*³⁴ have isolated the binuclear complex $[\{\text{VO}(\text{acpy-fah})\}_2(\mu\text{-O})_2]$ along with the non-separable mononuclear $[\text{VO}_2(\text{acpy-fah})]$ in minor amounts. However, the latter could only be characterized by single-crystal X-ray method.



The binuclear complexes exhibit one strong resonance at ≈ -509.3 ppm. In these complexes the two vanadium atoms, with distorted octahedral coordination, are bridged symmetrically through two oxo-

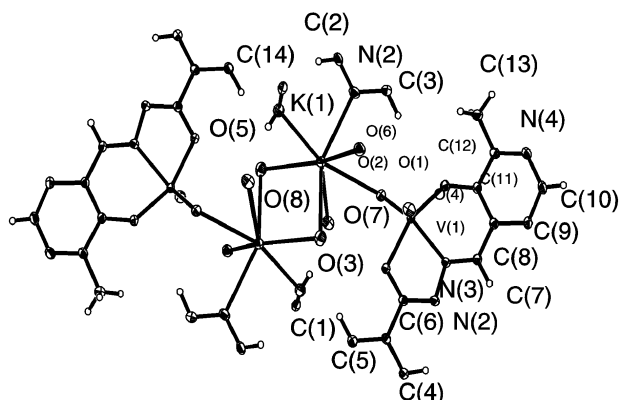


Figure 3. ORTEP plot (at 30% probability level) of $[\text{K}(\text{H}_2\text{O})_3][\text{VO}_2(\text{pydx-inh})]$.



Figure 4. ORTEP plot with 35% probability level of $[\text{VO}_2(\text{acpy-bhz})]$.

ligands. The vanadium centre in $[\{\text{VO}(\text{acpy-nah})\}_2(\mu\text{-O})_2]$ is in the plane surrounded by the three coordinating ligand functions (N1, N2, O3) and the symmetry-related bridging oxygen O2A (figure 5).

3. Reactivity of model complexes

3.1 Reactivity with H_2O_2

As mentioned in §1, haloperoxidases coordinate with peroxide to give η^2 -peroxo species. Such species have also been either isolated or generated in solution and characterized by spectroscopic study. Thus, treatment of a methanolic solution of $[\text{K}(\text{H}_2\text{O})][\text{VO}_2(\text{sal-inh})]$ with aqueous 30% H_2O_2 yields the peroxo complex $\text{K}[\text{VO}(\text{O}_2)(\text{sal-inh})(\text{H}_2\text{O})]$. Complex $\text{K}[\text{VO}(\text{O}_2)(\text{Cl-sal-inh})(\text{H}_2\text{O})]$ has also been isolated similarly. These complexes show three IR active vibrational modes associated with the $[\text{V}(\text{O}_2)]^{2+}$ moiety, namely the symmetric $\text{V}(\text{O}_2)$ stretch (ν_2) at ≈ 580 cm^{-1} , the antisymmetric $\text{V}(\text{O}_2)$ stretch (ν_3) at ≈ 740 cm^{-1} , and the $\text{O}-\text{O}(\nu_1)$ stretch at ≈ 895 cm^{-1} , characteristic of η^2 -coordination of the peroxo group. In addition, they display the $\nu(\text{V}=\text{O})$ mode at ≈ 950 cm^{-1} . These complexes are unstable and lose oxygen even at ambient temperature within a day. Formation of peroxo complexes in methanol by the treatment of 5 ml of $\approx 10^{-4}$ M solutions of $[\{\text{VO}(\text{sal-inh})\}_2\mu\text{-O}]$ with aqueous 30% H_2O_2 dissolved in methanol has been established by electronic absorption spectroscopy.²⁶ Thus, the band for $[\{\text{VO}(\text{sal-inh})\}_2\mu\text{-O}]$

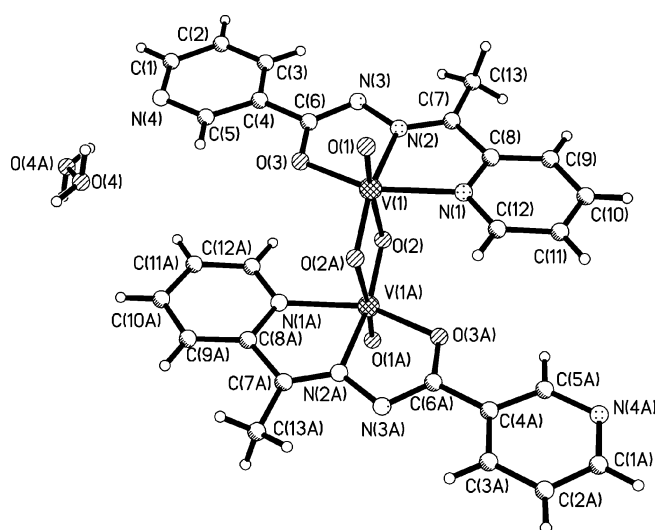


Figure 5. ORTEP plot (30% probability level) of $[\{\text{VO}(\text{acpy-nah})\}_2(\mu\text{-O})_2] \cdot 1.5 \text{H}_2\text{O}$.

inh) $\}_2\mu\text{-O}]$ at 402.5 nm shifts to 412 nm along with an increase in intensity. The new bands remain constant for several hours at approximately 10°C. The amount of peroxo complex formed depends upon the amount of H₂O₂ added. The final spectral pattern is similar to that obtained for the isolated peroxo complex $[\text{VO}(\text{O}_2)(\text{sal-inh})(\text{H}_2\text{O})]^-$. Similar spectral patterns are also observed for $[\text{K}(\text{H}_2\text{O})][\text{VO}_2(\text{sal-nah})]$ and $[\text{K}(\text{H}_2\text{O})][\text{VO}_2(\text{sal-fah})]$. The ⁵¹V NMR spectrum of $[\text{K}(\text{H}_2\text{O})][\text{VO}_2(\text{sal-fah})]$ in DMSO/H₂O plus a small amount of HClO₄ and H₂O₂, i.e. under conditions where the peroxo complexes should form and be fairly stable, resulted in the appearance of an additional peak at -575 ppm along with the original signal at -538 ppm.²⁸ The signal at -575 ppm reflects the presence of an oxomonoperoxo species. The peroxo ligand usually gives rise to an upfield shift of 40–60 ppm with respect to the parent dioxovanadium(V) complex.

Reaction of potassium vanadate with aqueous 30% H₂O₂ in presence of ligand H₂pydx-bhz (VI) also resulted in the formation of stable peroxo complex $\text{K}[\text{VO}(\text{O}_2)(\text{pydx-bhz})]$. Its formation in solution has also been established by electronic absorption spectroscopy (figure 6) by treating $[\text{VO}_2(\text{pydx-bhz})]^-$ with H₂O₂ in methanol. The band for $[\text{VO}_2(\text{pydx-bhz})]^-$ at 404.5 nm shifts to 424 nm along with increase in intensity on dropwise addition of H₂O₂, while the band at 329 nm shifts marginally to

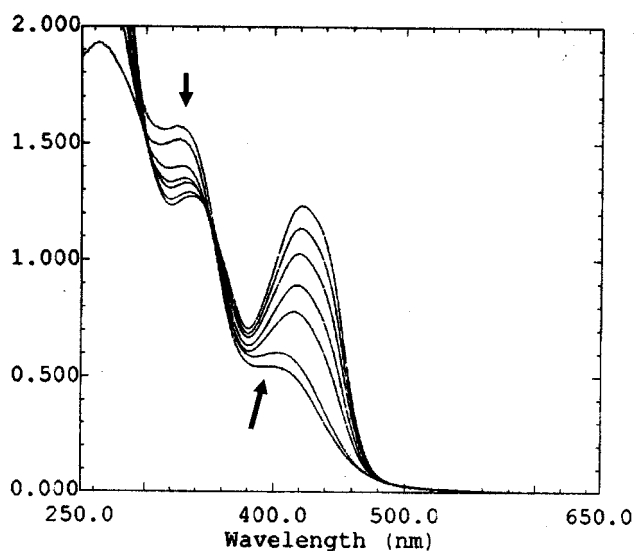


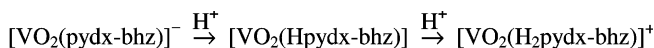
Figure 6. Titration of $[\text{K}(\text{H}_2\text{O})_2][\text{VO}_2(\text{pydx-bhz})]$ with 30% H₂O₂; the spectra were recorded after successive addition of 2-drop portions of H₂O₂ to 10 ml of a $\approx 10^{-4}$ M solution of complex in MeOH.

333 nm with partial reduction in intensity. The final spectrum is again similar to that obtained for the isolated peroxo complex $\text{K}[\text{VO}(\text{O}_2)(\text{pydx-bhz})]$.³¹

3.2 Reactivity with HCl

For the catalytic activity of vanadate-dependent haloperoxidases, the presence of a coordinated hydroxo ligand has been proposed on the basis of kinetic investigations. The generation of oxo-hydroxo species has been accomplished for $\{[\text{VO}(\text{sal-inh})\}_2\mu\text{-O}\}$ on reaction with HCl. Addition of HCl-saturated methanol to the methanolic solution of $\{[\text{VO}(\text{sal-inh})\}_2\mu\text{-O}\}$ results in a colour change from orange-red to dark red with a gradual shift of the bands at 322 and 402.5 nm to 341 and 425 nm respectively. Similar behaviour is also observed for $\{[\text{VO}(\text{Cl-sal-inh})\}_2\mu\text{-O}\}$ where the bands at 321.5 and 408.5 nm gradually shift to 337 and 428 nm on acidification. For complex $[\text{K}(\text{H}_2\text{O})][\text{VO}_2(\text{sal-fah})]$, the UV bands at 282.5, 301 and 324 nm finally merge into two bands at 300 and 318 nm, while a shoulder appears at ≈ 290 nm. These results have been interpreted in terms of the formation of oxo-hydroxo complexes of composition $[\text{VO}(\text{OH})(\text{HL})]$ via intermediate $[\text{VO}_2(\text{HL})]$ where one of the =N–N= nitrogens is the site of protonation. As mentioned in §2.1, the structurally characterized complex $[\text{VO}(\text{Hsal-bhz})]$ has protonated hydrazone nitrogen and is obtained on treatment of the corresponding anionic dioxo complex with HCl.²⁹

Complex $[\text{K}(\text{H}_2\text{O})_2][\text{VO}_2(\text{pydx-bhz})]$, provides results as shown in figure 7 and is again similar to those observed above. Corresponding results have also been obtained with HClO₄ (dissolved in a minimum amount of methanol) and added dropwise to a methanolic solution of $[\text{K}(\text{H}_2\text{O})_2][\text{VO}_2(\text{pydx-bhz})]$. These results have been interpreted in terms of the formation of an oxo-hydroxo complex of composition $[\text{VO}(\text{OH})(\text{H}_2\text{pydx-bhz})]^{2+}$ also but via $[\text{VO}_2(\text{Hpydx-bhz})]$ and $[\text{VO}_2(\text{H}_2\text{pydx-bhz})]^+$ on acidification as shown in scheme 5. The formation of the intermediate species, protonated at the pyridine-N, viz. $[\text{VO}_2(\text{Hpydx-bhz})]$, is based on the fact that electronic absorption spectrum of a solution of $[\text{K}(\text{H}_2\text{O})_2]$



Scheme 5.

[VO₂(pydx-bhz)] obtained after addition of 4 drops of HCl nearly matches the spectrum of the authentic complex [VO₂(Hpydx-bhz)]. The protonation of the N of the hydrazide moiety not involved in coordination is supplemented by a newly arising medium intensity band in the IR at 3205 cm⁻¹ (free Schiff base: 3210 cm⁻¹) on acidification of [K(H₂O)₂][VO₂(pydx-bhz)].³¹

3.3 Reactivity with noninnocent ligands

The ligands catechol and benzohydroxamic acid belong to this category and generally bind to vanadium

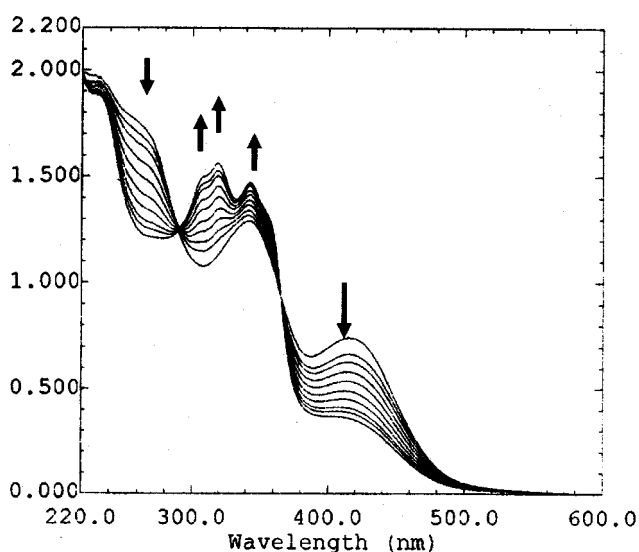
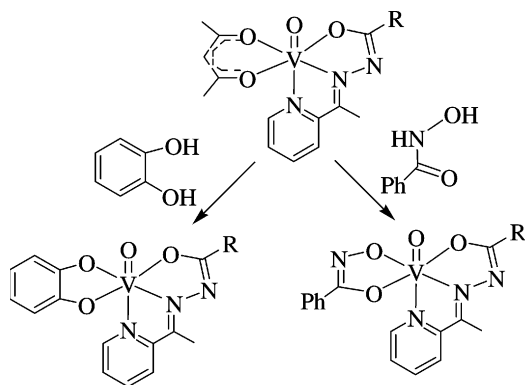


Figure 7. Titration of [K(H₂O)₂][VO₂(pydx-bhz)] with a saturated solution of HCl in MeOH; the spectra were recorded after addition of 2 drops portions MeOH-HCl to 10 ml of $\approx 10^{-4}$ M solution of complex in MeOH.



R = 3-pyridyl, 4-pyridyl, 2-furyl and ph.

Scheme 6.

in high-valent state. The relevance of catecholato-vanadium complexes in terms of their biological

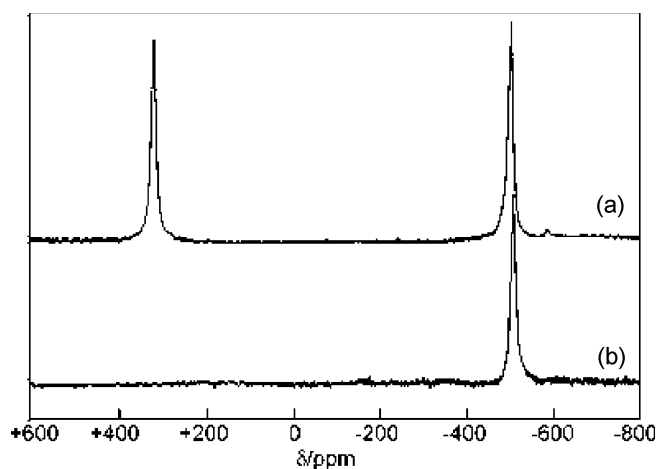


Figure 8. ⁵¹V NMR spectra of [VO(cat)(acpy-bhz)] (a) and [VO₂(acpy-bhz)] (b) recorded in DMSO-*d*₆.

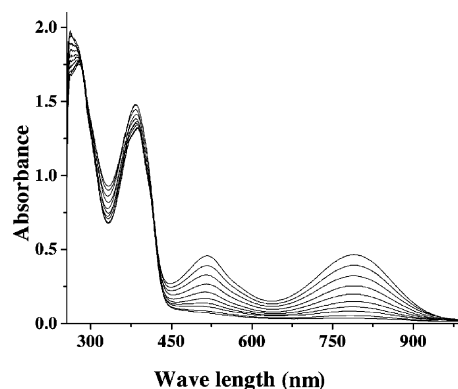


Figure 9. Decomposition of [VO(cat)(acpy-nah)] in 5 ml of DMSO after the addition of two drops of water, as a function of time.

Table 1. ⁵¹V NMR spectra data.

Complex	Chemical shift (δ in ppm)	
	Peak 1	Peak 2
[VO(cat)(acpy-inh)]	362.4	-506.9, -585.8
[VO(bha)(acpy-inh)]	70.0	-499.3, -587.7
[VO ₂ (acpy-inh)]	—	-507.1
[VO(cat)(acpy-bhz)]	319.1	-507.1, -589.2
[VO(bha)(acpy-bhz)]	51.2	-506.2, -590.2
[VO ₂ (acpy-bhz)]	—	-507.8
[VO(cat)(acpy-nah)]	343	-506.9
[VO(bha)(acpy-nah)]	66.5	-502.9
[{VO(acpy-nah)} ₂ (μ -O) ₂]	—	-509.3
[VO(cat)(acpy-fah)]	340	-513.5
[VO(bha)(acpy-fah)]	58.3	-505.7
[{VO(acpy-fah)} ₂ (μ -O) ₂]	—	-508.2

significance arises from the role of tunichromes in reduction, stabilization and accumulation of vanadium by certain ascidians (sea squirts). The iron-binding sidophore desferrioxamine, which contains hydroxamate functions, also strongly binds to VO^{2+} .

Reaction of catechol (H_2cat) or benzohydroxamic acid (H_2bha) with oxovanadium (IV) complex $[\text{VO}(\text{acac})(\text{acpy-inh})]$ in methanol under aerobic conditions leads to the formation of the mixed ligand complexes $[\text{VO}(\text{cat})(\text{acpy-inh})]$ and $[\text{VO}(\text{bha})(\text{acpy-inh})]$, respectively.³² During this reaction, oxidative replacement of the acetylacetonato group by catecholate or benzohydroxamate takes place as shown in scheme 6.

Similarly, oxovanadium(V) complexes $[\text{VO}(\text{cat})\text{L}]$ and $[\text{VO}(\text{bha})\text{L}]$, from the corresponding $[\text{VO}(\text{acac})\text{L}]$ (where HL = VIII, IX and X), have been prepared.³³ These complexes exhibit two resonances in their ^{51}V NMR spectra (table 1) and their representative ^{51}V NMR spectra of $[\text{VO}_2(\text{acpy-bhz})]$ and $[\text{VO}(\text{cat})(\text{acpy-bhz})]$ are presented in figure 8. Low-field signals between 319.1 and 362.4 ppm in catecholate and between 51.2 and 70.0 ppm in hydroxamate complexes (peak 1) are indicative of the catecholate/hydroxamate coordination and thus belong to the mixed-ligand complexes $[\text{VO}(\text{cat})\text{L}]$ and $[\text{VO}(\text{bha})\text{L}]$ respectively. The second peaks in the range -499.3 to -513.95 ppm (peak 2) are due to their partial decomposition to the corresponding dioxovanadium(V) complex. In some of the solutions, the presence of an additional minor resonance around -590 ppm matches with the corresponding oxoperoxo complexes.

The conversion of these mixed-chelate complexes into the $[\text{VO}_2]^+$ (peak 2) species with the loss of the bidentate catecholate (2-) and benzohydroxamate (2-) in DMSO was also established by electronic absorption studies. In dry DMSO, conversion is rather slow and requires about 24 h, while the addition of a few drops of water facilitates conversion. During this period, a gradual loss in intensity of the LMCT band(s) belonging to coordinated catecholate or benzohydroxamate is observed which finally disappears (figure 9).

4. Conclusions

At the active sites of vanadate-dependent haloperoxidases, vanadate has a trigonal-bipyramidal (native form) structure with O_4N coordination environment. Complexes reported in the present study partly model haloperoxidases. Intermediate species with

$\{\text{VO}(\text{H}_2\text{O})\}$, $\{\text{VO}_2\}$, $\{\text{VO}(\text{OH})\}$ and $\{\text{VO}(\text{O}_2)\}$, as postulated during catalytic turnover, have also been either isolated or generated in solution and characterized. Reactivity of the model complexes with various substrates, isolation of the resulting complexes, their characterization and stability in solution, has been studied.

Acknowledgements

Financial assistance from the Department of Science and Technology, New Delhi and the Council of Scientific and Industrial Research, New Delhi is gratefully acknowledged.

References

1. Pecoraro V L, Sleboznick C and Hamstra B 1998 *Vanadium complexes: Chemistry, biochemistry and therapeutic applications* (ACS Symposium Series) (eds) D C Crans and A S Tracy (Washington, DC: Am. Chem. Soc.) ch. 12
2. Rehder D 2003 *Inorg. Chem. Commun.* **6** 604
3. Sakurai H, Kojima Y, Yoshikawa Y, Kawabe K and Yasui H 2002 *Coord. Chem. Rev.* **336** 187
4. Thompson K H, McNeill J H and Orvig C 1999 *Chem. Rev.* **99** 2561
5. Maurya M R, Khurana S, Shailendra, Azam A, Zhang W and Rehder D 2003 *Eur. J. Inorg. Chem.* 1966
6. Ligtenbarg A G J, Hage R and Feringa B L 2003 *Coord. Chem. Rev.* **237** 89
7. Conte V, Furia F D and Licini G 1997 *Appl. Catal.* **A157** 335
8. Maurya M R, Kumar M, Titinchi S J J, Abbo H S and Chand S 2003 *Catal. Lett.* **97** 86
9. Maurya M R, Saklani H, Kumar A and Chand S 2004 *Catal. Lett.* **93** 121
10. Maurya M R, Kumar A, Manikandan P and Chand S 2004 *Appl. Catal.* **A45** 277
11. Maurya M R, Saklani H and Agarwal S 2004 *Catal. Commun.* **5** 563
12. Butler A 1999 *Bioinorganic catalysis* 2nd edn (eds) J Reedijk and E Boiwmann (New York: Marcel Dekker) ch. 5
13. Butler A 1999 *Coord. Chem. Rev.* **187** 17
14. Rehder D 2001 *J. Inorg. Biochem.* **80** 133
15. Janas Z and Sobota P 2005 *Coord. Chem. Rev.* **249** 2133
16. Weyand M, Hecht H J, Keiß M, Liaud M F, Vilter H and Schomburg D 1999 *J. Mol. Biol.* **293** 595
17. Isupov M I, Dalby A R, Brindley A A, Izumi Y, Tanabe T, Murshudov G N and Littlechild J A 2000 *J. Mol. Biol.* **299** 1035
18. Messerschmidt A and Wever R 1996 *Proc. Natl. Acad. Sci. USA* **93** 392
19. Kuchta L, Sivak M, Marek J, Pavelcik F and Cäsny M 1999 *New J. Chem.* **23** 43
20. Messerschmidt A, Prade L and Wever R 1997 *Bio. Chem.* **378** 309

21. Franssen M C R 1994 *Biocatalysis* **10** 87
22. (a) Franssen M C R 1994 *Catal. Today* **22** 441; (b) Colpas G J, Hamstra B J, Kampf J W and Pecoraro V L 1996 *J. Am. Chem. Soc.* **118** 3469; (c) Hamstra B J, Colpas G J and Pecoraro V L 1998 *Inorg. Chem.* **37** 949
23. Satoni G, Licini G M and Rehder D 2003 *Chem. Eur. J.* **9** 4700
24. Smith T S II and Pecoraro V L 2002 *Inorg. Chem.* **41** 6754
25. Maurya M R 2003 *Coord. Chem. Rev.* **237** 163
26. Maura M R, Khurana S, Schulzke C and Rehder D 2001 *Eur. J. Inorg. Chem.* 779
27. Rehder D 1992 *Transition metal nuclear magnetic resonance* (ed.) P S Pregosin (New York: Elsevier) p. 1
28. Maurya M R, Agarwal S, Bader C, Ebel M and Rehder D 2005 *Dalton Trans.* 537
29. Plass W, Pohlmann, A and Yozgatli H K 2000 *J. Inorg. Biochem.* **80** 181
30. Hirao T 1997 *Chem. Rev.* **97** 2707
31. Maurya M R, Agarwal S, Bader C and Rehder D 2005 *Eur. J. Inorg. Chem.* 147
32. Maurya M R, Khurna S, Zhang W and Rehder D 2002 *Eur. J. Inorg. Chem.* 3015
33. Maurya M R, Agarwal S, Abid M, Azam A, Bader C, Ebel M and Rehder D 2006 *Dalton Trans.* 937
34. Deflon V D, De Oliveira D M, de Sousa G F, Batista A A, Dinelli L R and Castellano E E 2002 *Z. Anorg. Allg. Chem.* **628** 140